TEKA. COMMISSION OF MOTORIZATION AND ENERGETICS IN AGRICULTURE – 2014, Vol. 14, No.2, 179-189

Modelling of electromagnetic processes in ferromagnetic screens shorted winding asynchronous motor-fan with two rotor package using program complex FEMM 3.4

Igor Zakharchuk

Volodymyr Dahl East-Ukrainian University,
Molodzhny bl., 20a, Lugansk, 91034, Ukraine, e-mail: e-mail: rty@lds.net.ua

Received May 28.2014: accepted June 06.2014

S u m m a r y . Defined active and inductive resistances of the rotor winding through the simulation of electromagnetic processes in ferromagnetic screens shorted winding asynchronous motor-fan with two rotor package using program complex FEMM 3.4.
K e y w o r d s : asynchronous motor-fan, simulation of electromagnetic processes, ferromagnetic screens.

INTRODUCTION

Locomotives operated on the possibility of using the effective power of the diesel engine for traction work is far from being full. So existing diesel locomotives directly transmitted to the wheels only (0.73-0.76) efficient diesel power. The rest of the power consumed by losses in electrical transmission, the drive mechanisms and auxiliary diesel engine cooling.

On diesel engines, cooling of diesel is carried out by a relay method by means of including and disconnecting of asynchronous motor-fans (AMF).

This part of the standard freight locomotive type 2TE116 capacity of 2200 kW per section for passenger locomotives TEP150 capacity of 3100 kW. When the relay cooling occur: temperature fluctuations coolants, heavy starting conditions motor-fans, a significant power consumption by fan drive to operate a diesel locomotive at ambient temperatures below +40°C and no nominal operating conditions of diesel. For the increase of economy of the system of cooling of diesel it is expedient to apply the continuous adjusting of frequency of rotation of fans [13, 14].

This is because the volume of air that is supplied by a motor-fan for cooling diesel depends on first power of the rotational speed and the shaft power of the fan depends on the third power of the speed.

General Electric Company in locomotives with index 8 (B23-8, B30-8, C30-8, B36-8, C36-8, etc.) replaces mechanical fan drives on two DC motor power 44 kW, speed of each run power semiconductor regulators function of water temperature at the outlet of the diesel engine. As a result, average operating power consumption by fan drive down 60%.

Company General Motors replaced in locomotives SD series three one speed AMF capacity of 29.6 kW diesel on two speed. Application of two-speed AMF compared with single-speed diesel locomotives series SD

2940 kW capacity gives fuel savings of 7.6 to 12.5 thousand liters per year.

Consequently, the development and introduction of more fuel-efficient locomotives for cooling systems for diesel engine with continuously adjustable electrically operated fan is very timely.

On new diesel engines for diminishing of expenses of energy on cooling of diesel the managed is offered the change of voltage on the winding of stator asynchronous motor-fan with a two package rotor with ferromagnetic screens in short-circuited winding of rotor. It promotes pure resistance of winding of rotor and provides good regulation descriptions.

An asynchronous motor-fan with a two package rotor (Fig. 1) contains stator 1 with a winding and stator core, connected with foundation 2 by a hob 3, which carries the supporting bearings 4. Shaft 5 connected with a rotor by a butt-end shield 6.

A rotor is executed a two package with two short-circuited winding for the increase of pure resistance of winding of rotor. One package of rotor is contained by bars 7 and 8, external rings 12 and internal rings 13. Rings 12 and 13 short-circuit short-circuited bars 7, 8. A rotor contains a wheel 9, on which blades are fastened 10. There are butt-end ferromagnetic screens 11 for rings 12 and 13. Screens engulf rings.

Between ferromagnetic screens 14 there is a circular vent slot 15. Internal ferromagnetic screens 14 cool down through openings 16 in foundation 2, through openings 17 in the lower package of stator 1, through the slots of explorers of winding stator between two packages of stator, through a circular slot 15 between internal screens 14, through openings 18 in a wheel 9. External ferromagnetic screens 11 cool down from blades 10.

Magnetic fields of dispersion of rings 12 and 13 winding of two package rotor induce eddy currents in the ferromagnetic screens of rings 11 and 14 and create additional losses in screens 11 and 14, that increases equivalent active resistance of rotor.

Ferromagnetic screens 11 cool down the current of air of blades 10. Ferromagnetic screens 14 cool down through vent openings 16, 17, 18 and circular slot 15. A thermal stream, that goes from a rotor to stator 1 with two by laminated packages, goes down, the winding of статора does not overheat. Due to it reliability of work of motor-fan rises in the wide turn-down of sliding.

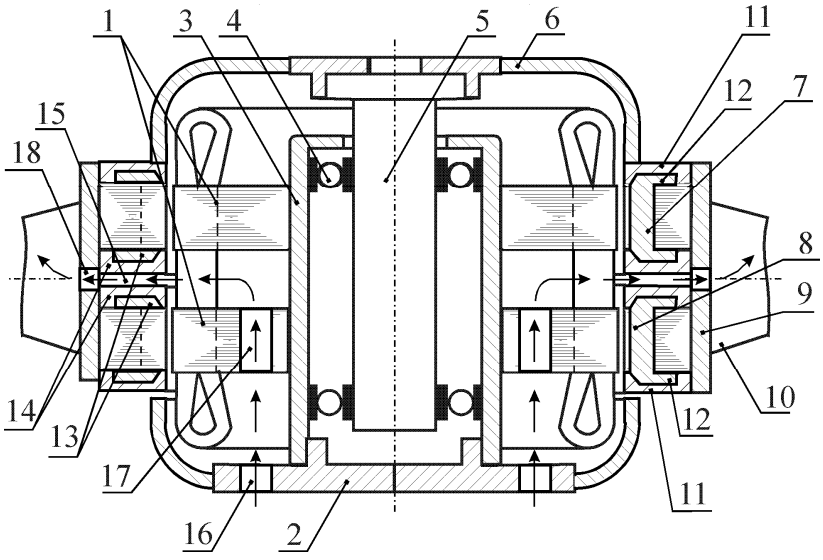

Fig. 1. Construction of asynchronous motor-fan with the screened short-circuited rings in of rotor winding with a two package rotor

A two package rotor with two short-circuited windings is needed for the additional increase of active resistance of rotor winding from additional internal short-circuited rings 13 with ferromagnetic screens 14 for motor-fans with the number of poles more than 4.

Internal screens 14 can absent.

Voltage on stator diminish for adjusting of rotation speed of motor-fan. Rotation speed of motor-fan diminishes. Sliding of rotor is increased. Frequency of current is increased in the rotor winding. Frequency of eddy currents is increased in ferromagnetic screens 11. Additional losses are created in a rotor and active resistance of rotor is increased. Stiffness of mechanical characteristics is reduced. Stable operation of the motor-fan is provided in the range of variation of the slip from $s = s_r$ to $s = 1$.

Active and inductive resistances of rotor winding must be defined for the calculation of mechanical and regulation characteristics of motor-fan.

The method of calculation of active and inductive resistances of rotor winding is developed taking into account losses in ferromagnetic screens. Losses in ferromagnetic screens determined by solving the equations of the electromagnetic field in ferromagnetic elements winding (in screens) rotor.

Analytical methods for solving equations of the electromagnetic field in ferromagnetic elements of rotor windings differ generality and clarity of the solutions obtained. Particularly deep analytical methods developed for induction motors with solid rotors [8, 20, 9, 16] and two-layer rotors [12, 11, 15, 17, 3].

The analytical methods of calculation of the electromagnetic field in ferromagnetic bodies are based on the row of assumptions: 1) constancy of permeability of environment, 2) assumption of a sudden manifestation of the skin effect, 3) hyperbolic distributing of permeability on the depth of array, 4) account only by the tangential constituent of the magnetic field. These methods give acceptable integral characteristics of the field and parameters of massive ferromagnetic environment [2, 19].

Application of numeral methods considerably extends possibilities of research of processes in ferromagnetic elements, allows to take into account non-linearity of environment a task the known dependence $B(H)$ [10].

To date, accurately enough electromagnetic field calculation possible using numerical methods, in particular, the finite element method (FEM). To calculate the two-dimensional fields of finite element method known the following: licensed version ELCUT [1] and the free version of FEMM 3.4 [4].

OBJECT OF RESEARCH

A research object is distributing of the electromagnetic field in the ferromagnetic screens of rotor for determination of active and inductive resistances of rotor winding.

PURPOSE OF RESEARCH

The purpose of this study is modelling of electromagnetic processes in ferromagnetic screens shorted winding of rotor asynchronous motor-fan with two package rotor using FEMM 3.4 software. On results the calculation of the magnetic field in a screen determine active and reactive powers in a screen for determination of active and inductive resistances of the rotor winding.

RESULTS OF RESEARCH

For the calculation of descriptions of motor-fan it is necessary to define active and inductive resistances of rotor winding for one package. A rotor will present as a polyphase winding. The number of phases is equal to the number of bars of rotor winding. The number of pair of poles of rotor winding is equal to the number of pair of poles of stator winding.

Active r_2 and inductive x_2 resistances of rotor winding for one package are determined [21]:

$$r_2 = r_b + \frac{r_{rs}}{2\sin^2\frac{\pi p}{z_2}}, x_2 = x_b + \frac{x_{rs}}{2\sin^2\frac{\pi p}{z_2}},$$

where: r_b and x_b – active and inductive resistances of bar 7 (Fig. 1) determined ordinary a way [6],

r_{rs} and x_{rs} – active and inductive resistances of short-circuited ring 12 with a screen 11,

z_2 – number of slots of rotor.

Will define active and inductive resistances of area of short-circuited ring of rotor winding between two bars with a ferromagnetic screen taking into account the skin effect by using complex software FEMM 3.4 [1, 4].

The geometrical sizes of screen followings: height h (on a co-ordinate y), thickness b (on a co-ordinate z). Middle diameter of ring D_{rs}, length l_r of ring (between two nearby bars of rotor, on a co-ordinate x):

$$l_r = \frac{\pi D_{rs}}{z_2}. \quad (1)$$

On a (Fig. 2) calculation chart is resulted for the real area of short-circuited ring with a ferromagnetic screen between two bars of rotor winding.

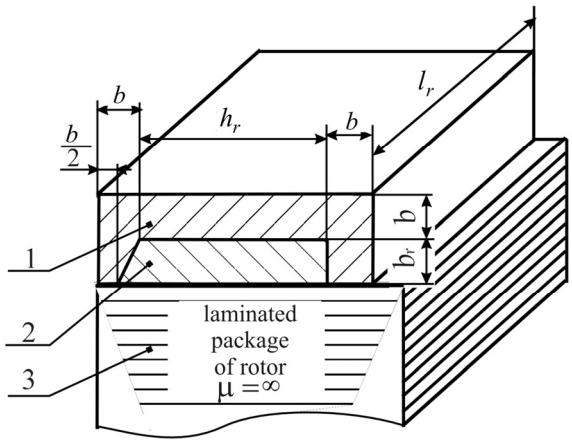

Fig. 2. Area of short-circuited ring with a ferromagnetic screen between the bars of rotor: 1 – ferromagnetic screen, 2 – short-circuited ring of rotor winding, 3 – laminated package of rotor, b_r and h_r – width and height of ring, l_r – length of area of ring between the bars of rotor winding, b – a thickness of ferromagnetic screen

Calculation of the magnetic field in the screen by the method of finite elements in axisymmetric formulation of the problem. (Fig. 3, a) shows the block diagram for the site shorting ring with a ferromagnetic screen between two bars of the rotor winding. The basic equation for the calculation of the magnetic field has the form [1, 6]:

$$\frac{\partial}{\partial r}\left(\frac{1}{r\mu_z}\frac{\partial(rA)}{\partial r}\right)+\frac{\partial}{\partial z}\left(\frac{1}{r\mu_r}\frac{\partial A}{\partial z}\right)-\frac{i\omega A}{\rho_r}=-j \quad (2)$$

where: A – complex vectorial magnetic potential,

r, z – normal vectors on a radius and on an axis,

ρ_r – specific active resistance,

μ_z, μ_r – vectors of permeability,

ω – angular frequency of the current,

j – external current density.

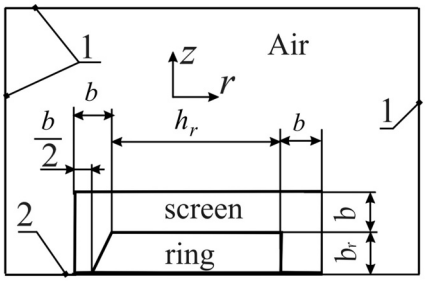

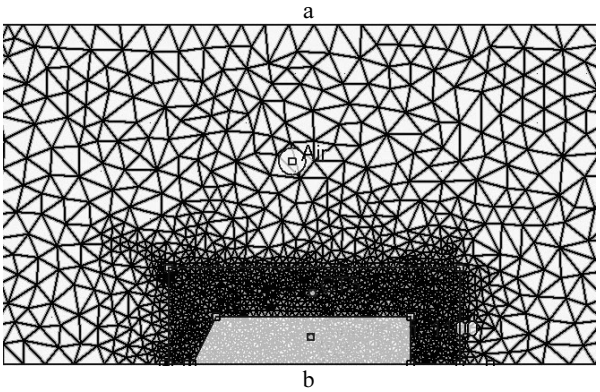

Fig. 3. Computational domain (a) and finite-element mesh (b) to calculate the magnetic field of short-circuited ring with a ferromagnetic screen

The followings assumptions are accepted:

1) the field in a screen is axisymmetric,

2) the external magnetic field of screen absents,

3) the currents of stator winding do not influence on the field of ring with a ferromagnetic screen,

4) the laminated core of rotor is unsaturated, therefore permeability is equal to endlessness,

5) material of screen is izotropic characteristics $\mu_r = \mu_z = \mu_{rs}$,

6) ignore the phenomenon of hysteresis in a screen.

The followings scope terms are accepted:

1) on a border 1(Fig. 3, a) condition of Dirichlet on a border-vectorial magnetic potential is equal to the zero (*A=0*),

2) on a border 2 (Fig. 3, a) border condition of Neyman – the normal derivative of vectorial magnetic potential is equal to the zero $\frac{\partial A}{\partial n} = 0$ [14].

For the calculation of the magnetic field the followings materials were chosen in obedience to the (Fig. 3, a): a screen is steel of St3, a ring is an aluminium alloy of AK12M4 with a current. The curve of dependence of H (B) is synonymous and determined dependence for steel of St3 [7]:

$$H = B\left(8{,}2 + \left(0{,}886|B|\right)^{8{,}6}\right). \quad (3)$$

Computational grid with triangular finite elements of the first order is shown in (Fig. 3, b). Calculations of the magnetic field carried by a free version of the program FEMM 3.4.

On results the calculation of the magnetic field in a screen determine complete S_s power by FEMM 3.4, selected in a screen. Determine also active and reactive constituents of current in a screen, which the power-factor of screen is determined from, that allows to expect active P_s and reactive Q_s powers in a screen.

Currents in a short-circuited ring and ferromagnetic screens are different, therefore their active and inductive resistances at determination of general resistance of ring with a screen must be resulted to one current.

Calculation active resistance r_{rs} of short-circuited ring of rotor winding with a screen for one package, determined on condition of equality of active powers, selected in resistance r_{rs} from a current I_r in the screened short-circuited ring and separately in a ring and in a ferromagnetic screen:

$$I_r^2 \cdot r_{rs} = I_r^2 \cdot r_r + P_s, \quad (4)$$

from where follows:

$$r_{rs} = r_r + \frac{P_s}{I_r^2}, \quad (5)$$

where: r_r – active resistance of area of ring between nearby bars.

Calculation inductive resistance x_{rs} of short-circuited ring of rotor winding with a screen will get like (4) on equation:

$$I_r^2 \cdot x_{rs} = I_r^2 \cdot x_r + Q_s, \quad (6)$$

$$x_{rs} = x_r + \frac{Q_s}{I_r^2}, \quad (7)$$

where: x_r – inductive resistance of area of ring between nearby bars.

In the absence of the inductive reactance of the screen ring from external leakage flux is determined [4]:

$$x_{rse} = 9{,}1 \cdot f \cdot l_r \cdot 10^{-6} \cdot \lg \frac{4{,}7 \cdot l_r}{\pi\left[\left(h_r + 2b_s\right) + \left(b_r + b_s\right)\right]}. \quad (8)$$

Active resistance of area of ring from [21]:

$$r_r = r_{ro}\lambda_r \frac{\left(ch2\lambda_r + \cos 2\lambda_r\right)\left(sh2\lambda_r + \sin 2\lambda_r\right)}{sh^2 2\lambda_r + \sin^2 2\lambda_r}, \quad (9)$$

inductive resistance of area of short-circuited ring from [21].

$$x_r = r_{ro}\lambda_r \frac{\left(ch2\lambda_r + \cos 2\lambda_r\right)\left(sh2\lambda_r - \sin 2\lambda_r\right)}{sh^2 2\lambda_r + \sin^2 2\lambda_r}, \quad (10)$$

where: r_{ro} – resistance of area of ring to the direct current:

$$r_{ro} = \frac{\rho_r l_r}{b_r h_r}. \quad (11)$$

$$\lambda_r = \frac{b_r}{\Delta_r}, \tag{12}$$

$$\Delta_r = \sqrt{\frac{2\rho_r}{\omega\mu_r}}, \tag{13}$$

where: Δ_r – depth of penetration of electromagnetic wave in the short-circuited ring of rotor winding.

Using on the software FEMM 3.4 in a table 1 and tabl2 2 active P_s and reactive Q_s powers of ferromagnetic screen are expected depending on frequency and value of current I_s in the screened short-circuited ring. The sizes of screen are resulted on a (Fig. 4).

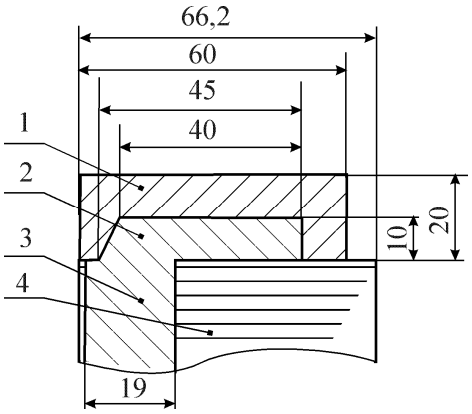

Fig. 4. Construction of short-circuited ring of rotor winding with a ferromagnetic screen for AMF by power 75 kW with the number of poles 8:
1 – ferromagnetic ring-screen from steel of St3,
2 – short-circuited ring,
3 – bar of rotor winding from an aluminium alloy,
4 – lamineted package of rotor from steel 2411

According to the results of theoretical analysis of electromagnetic processes in AMF with two package rotor simulation algorithm developed motor-fan with two packet rotor for steady-state modes. Determined according to: speed n or slip s, consumption current I_1, efficiency η, power factor $\cos\varphi$ on the value of the phase voltage U_{ph} on the stator winding. Parameters are calculated on a PC on the developed program in a language C^{++} that uses the results presented in (Table 1) and (Table 2).

Table 3 shows a comparison of calculated and experimental data for the motor-fan (nominal power of 75 kW) with the number of poles $2p$=8 on both the rotor and the packet with one screen on every package. When calculating the time of useful features for changing the fan wheel takes the square of the speed, which is slightly different from reality at low speeds.

From (Table 3) follows:

1) for nominal operation mode AMF error in determining consumption current does not exceed 3.9% slip – 3.3% efficiency – 0.59%,

2) by adjusting with the highest accuracy simulated sliding AMF – 10%.

Table 1. Results of calculation of active power P_s on the area of ferromagnetic screen (W) between the bars of rotor

Current in a ring, A	Frequency of current in a ring, Hz					
	5	25	45	65	85	105
200	0.32	0.72	0.96	1.12	1.32	1.44
600	1.80	3.96	5.40	6.48	7.20	8.28
1000	4.00	9.00	12.00	14.00	16.00	18.00
1400	5.88	15.68	19.60	23.52	27.44	31.36
1800	6.48	22.68	29.16	35.64	42.12	45.36
2200	9.68	33.88	38.72	48.40	53.24	62.92
2600	6.76	40.56	54.08	60.84	74.36	81.12
3000	9.00	54.00	72.00	81.00	90.00	99.00
3400	11.56	69.36	80.92	92.48	104.04	115.60
3800	14.44	72.20	101.08	115.52	129.96	144.40

Table 2. Results of calculation of reactive power Q_s on the area of ferromagnetic screen (VAr) between the bars of rotor

Current in a ring, A	Frequency of current in a ring, Hz					
	5	25	45	65	85	105
200	0.32	0.72	0.96	1.12	1.32	1.44
600	2.16	3.96	5.40	6.48	7.20	8.28
1000	5.00	9.00	12.00	14.00	16.00	18.00
1400	9.80	13.72	19.60	23.52	27.44	31.36
1800	12.96	22.68	29.16	35.64	42.12	45.36
2200	19.36	29.04	38.72	48.40	53.24	62.92
2600	20.28	40.56	54.08	60.84	74.36	81.12
3000	27.00	54.00	63.00	81.00	90.00	99.00
3400	34.68	69.36	80.92	92.48	104.04	115.60
3800	43.32	86.64	101.08	115.52	129.96	144.40

Table 3. Comparative analysis of theoretical and experimental data AMF75-2P-8 at a frequency of 100 Hz* voltage

Phase voltage, U_{pf}, V	Phase current, I_1, A		Error, %	Slip, s, %		Error, %	Efficiency, $\eta_{ме}$, %		Error, %
	Calculation	Experiment		Calculation	Experiment		Calculation	Experiment	
230	173	180	-3.9	6.12	6.1	3.3	84.9	84.4	0.59
200	189	199	-5.0	9.29	9.8	-5.2	81.7	80.8	1.11
180	204	216	-5.6	14.1	15.7	-10.0	77.5	74.6	3.9
160	224	230	-2.6	23.0	25.3	-9.0	68.3	64.5	5.9
140	223	219	1.8	37.8	36.7	3.0	51.8	53.5	-3.2
120	193	194	-0.5	51.8	48.6	6.6	38.5	42.3	-8.9
100	158	159	-0.6	62.8	60.3	4.0	29.1	32.3	-9.8
80	120	122	-1.6	71.2	68.7	3.6	22.2	24.6	-9.6
64	98	100	-2.0	80.5	77.9	3.3	14.8	16.3	-9.4

* Note. At rated speed 1405 r / min useful power AMF 73.4 kW.

Increased accuracy in determining the efficiency to 10% for large slides (at low speeds) can be attributed to some mismatch of real characteristics of the fan load torque resistance of the estimated quadratic.

The results of calculation of the magnetic field of the pictures in the ferromagnetic screen shown in (Fig. 5-8), which show that the magnetic field is concentrated mainly in the ferromagnetic screen, so the assumption holds no boundaries for its screen, namely in the air and a shorting ring. The figures also show that at higher sliding rotor, a more sharp manifestation of the skin effect in a ferromagnetic screen, and consequently an increase in resistance of the screen while reducing the speed by varying the voltage on the stator winding.

Fig. 9 shows the calculated dependence of consumption current I_1 and the slip s of the supply voltage U_{ph} at f_1 = 100 Hz for AMF 75 kW with different design of the rotor winding of aluminum alloy AK12M4: one package without ferromagnetic rotor screens, one package rotor with ferromagnetic screens, two package rotor without ferromagnetic screens, a rotor with a locking ring screened in each package two rotor windings.

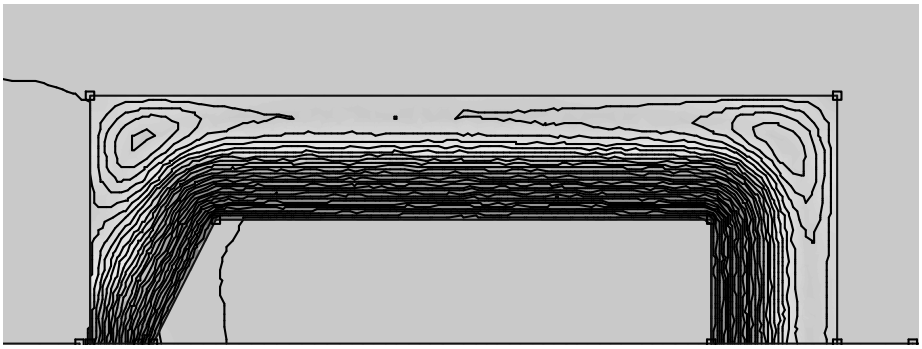

Fig. 5. Distribution power lines and the magnetic field in the ferromagnetic screen for motor-fan AMF75-2P-8 at a supply voltage of 230 V, 100 Hz and the rotor slip 6.1% (frequency current in the ring 6.1 Hz, the current in the ring 1324 A)

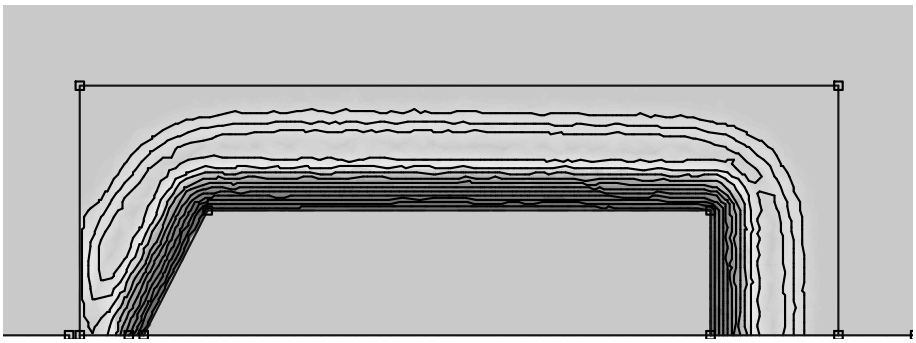

Fig. 6. Distribution of field lines and the magnetic field in the ferromagnetic screen for motor-fan AMF75-2P-8 at a supply voltage of 160 V, 100 Hz and rotor slip 23% (current frequency 23 Hz in the ring, the ring current 1888 A)

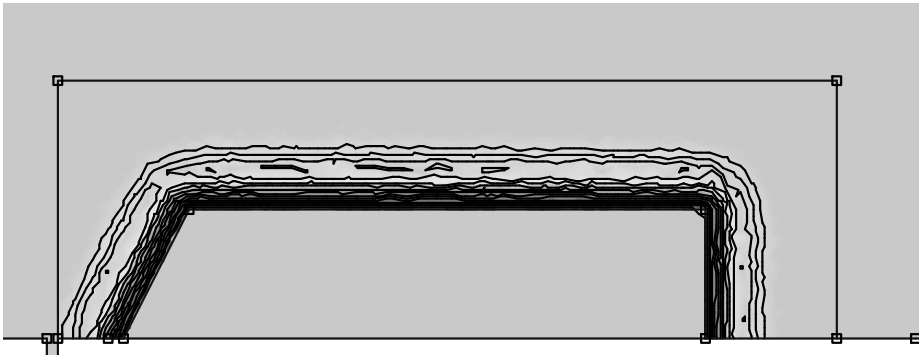

Fig. 7. Distribution of field lines and the magnetic field in the ferromagnetic screen for motor-fan AMF75-2P-8 at a supply voltage of 100 V, 100 Hz and the rotor slip 62.8% (current frequency of 62.8 Hz in the ring, the ring current 1331 A)

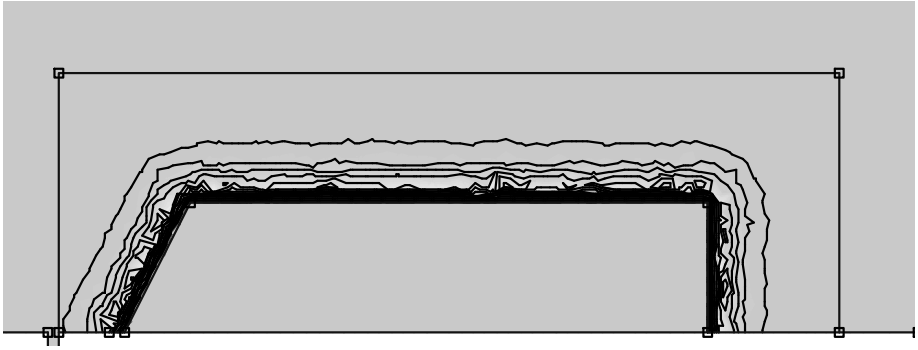

Fig. 8. Distribution of field lines and the magnetic field in the ferromagnetic screen for motor-fan AMF75-2P-8 at a supply voltage of 30 V, 100 Hz and rotor slip 93% (current frequency 93 Hz in the ring, the ring current is 245 A)

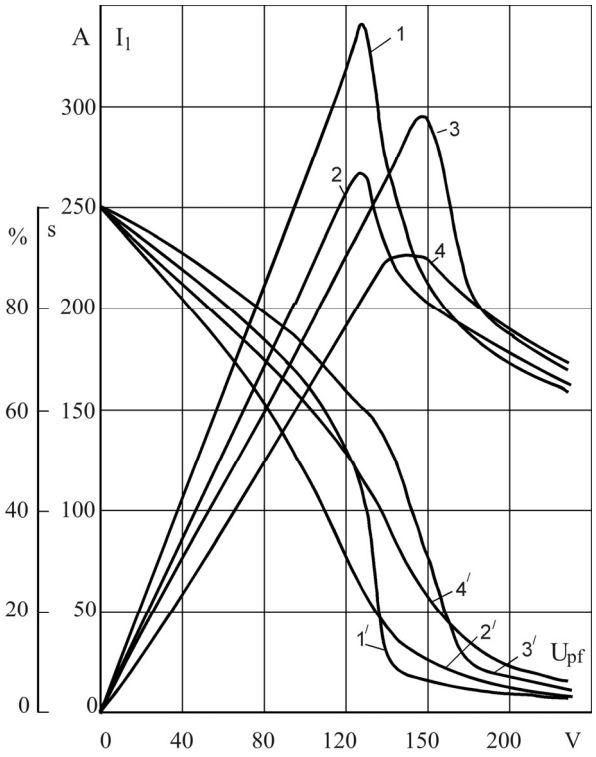

Fig. 9. Dependencies consumption current I_1 (1-4) and the slip s (1′ - 4′) of AMF from the supply phase voltage U_{ph}:

1, 1′ – one package without ferromagnetic rotor screens,

2, 2′ – one package with ferromagnetic rotor screens,

3, 3′ – two package rotor without ferromagnetic screens,

4, 4′ – with a rotor end ring screened in each package two rotor windings

Table 4 shows the calculated nominal data compared variants.

From (Fig. 9) and (Table 4) that AMF with one shielded locking ring in each winding rotor has two batch most favorable control characteristics $s = f(U_{ph})$, the maximum input current I_1 exceeds the nominal 27%, but this option is AMF in nominal mode has reduced the efficiency values and $\cos\varphi$.

Fig. 10 shows the dependence of the active $\bar{r}_{rs}$, inductive $\bar{x}_{rs}$ resistances shielded rings and the penetration depth of the electromagnetic wave (current) Δ_s from sliding (speed control AMF voltage changes), which were determined by the dependences obtained in the (Eg. 5), (Eg. 7), (Eg. 9) with algorithm simulation according to Annexes A and program developed in C^{++}.

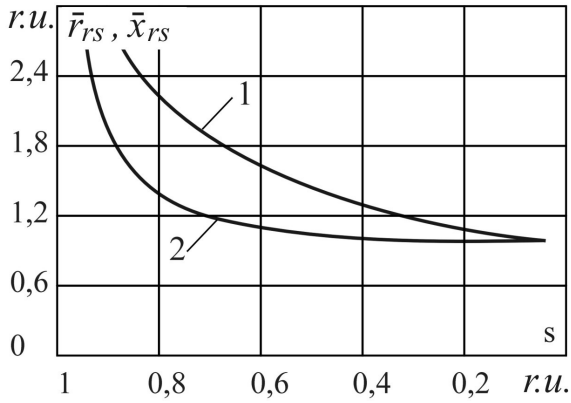

Fig. 10. Dependencies relative parameters of the rotor slip (speed control AMF voltage change):

1 – active resistance $\bar{r}_{rs} = r_{rs} / r_{rsr}$,

2 – inductive reactance $\bar{x}_{rs} = x_{rs} / x_{rsr}$,

3 – penetration depth of the electromagnetic wave shield $\bar{\Delta} = \Delta_s / b_s$

Rotor parameters r_{rsr}, x_{rsr} for the nominal mode, determined at $U_{ph} = 230\ V$ and sliding $s_r = 0{,}061$.

Table 4. Comparative analysis of nominal modes AMF with different design of the rotor at a frequency of 100 Hz and supply voltage 230 V

Variant of AMF	Current, I_1, A	Slip, s,%	Efficiency, η, %	Power factor, $cos\varphi$, r.u.	Useful power, P_2, kVA
One package of ferromagnetic rotor without screens	160	2.47	88.0	0.773	75.1
One package rotor with ferromagnetic screens	161	3.28	87.3	0.772	75.1
Two packages rotor without ferromagnetic screens	171	4.28	86.7	0.732	75.0
Rotor with a shielded locking ring in each package two rotor winding	173	6.12	84.9	0.727	73.4

CONCLUSIONS

1. As follows from (Fig. 10) in deep regulation for large slides active and inductive resistances shielded rotor rings increase 3 times, and the depth of the current flow Δ_s in the screen also significantly reduced due to the influence of the skin effect in a ferromagnetic screen.

2. Results shown in (Fig. 9), in the (Table 4) and in (Fig. 10), make it appropriate shielding rings rotor winding to improve the control characteristics of the asynchronous motor-fan when the voltage on the stator.

3. Comparative analysis of steady-state performance with different AMF rotor design identified (Fig. 9) that one package of motor-fan designs without serial ferromagnetic screens largely unregulated, i.e, significantly increasing the slip from 20% to 55% when the total voltage from 140 V to 120 V. The current consumption is increased to 340 A, which is unacceptable. Motor- fan with a shielded locking ring in each winding rotor has two package adjusting most favorable properties: slip varies smoothly, the current exceeds the maximum current at rated voltage of not more than 27%.

REFERENCES

1. **Belov V., Shabanov G., Karpushkina S., 2001.:** Mathematical modeling. Saransk University of Mordovia, 2001. 338. (in Russian).
2. **Brynskikh E., Danilevich Y., Yakovlev V., 1979.:** Electromagnetic fields in electrical machines. Leningrad: Energiya, 1979. 152. (in Russian).
3. **Chalmers B., Ilandi E., 1983.:** Analysis of Induction machines with unlaminated steel sections by multilayer transformatrix method. Collog. Probl. Model.Non-Linear.: Educ. and Tecnol. Div. Profess. Group. S.B. London. 14-25.
4. **David Meeker.** User's Manual. Finite Element Method Magnetics. Version 3.4. / David Meeker. source: http:femm.info/Archives/doc/manual34.pdf.
5. **Dzetcina O., Fedorchenko V., 2011.:** On the issue of energy efficiency of industrial locomotives. TEKA Commission of Motorization and Power Industry in Agriculture, V. XI A, 69-77.
6. **Kopylov I., 1996.:** Mathematical modeling of electrical machines. Moscow Graduate School, 1996. 318. (in Russian).
7. **Kopylov I., Klokov B., Morozkin V., 1996.:** Design of electrical machines: Proc. vuzov. In 2 books.: kn.1 Energoatomizdat, 1993. 464. (in Russian).
8. **Kutsevalov V., 1979.:** Asynchronous and synchronous machines with massive rotors. Moscow: Energiya, 1979. 212. (in Russian).
9. **Kutsevalov V.M., 1979.:** Asynchronous and synchronous machines with massive rotors. Moscow, Energiya, 212. (in Russian).
10. **Lischenko A., Lesnik V., 1984.:** Asynchronous machine with a massive ferromagnetic rotor. Kyiv. Naukova dumka, 168. (in Russian).
11. **Martynov V., Olejnikov A., Belyaeva L., 2001.:** The current distribution in the array double-layer rotor induction motor . Optim. Mfr. processes: Sat scientific. tr. Sevastopol Reg. tehn. Univ. Sevastopol. 135-139. (in Russian).
12. **Mogilnikov V., Olejnikov A., 2008.:** Theory, technology and modes of operation of induction motors with two-layer rotor: monograph. Sevastopol Univ SevNTU. 350. (in Russian).
13. **Mohyla V., Sklifus Y., 2010.:** The prospects of increasing the effectiveness of the cooling device of a diesel locomotive. TEKA Commission of Motorization and Power Industry in Agriculture, V. XC. 198-203.
14. **Neumann, L., Demirchyan K., 1981.:** Theory of Electrical Engineering: In 2 volumes textbook for high schools. Tom 2. L. Energoizdat. 426. (in Russian).
15. **Olejnikov A., Smirnov S., Safronov A,. 1994.:** Features electromagnetic processes and relations in blood pressure with two-layer rotor for EA with parametric control. Electricity. № 11. 18-25. (in Russian).
16. **Olejnikov A., Smirnov S., Safronov A., 1993.:** Mathematical modeling of energy processes in induction machines with distributed parameters, taking into account the nonlinearity of the rotor. Electronic automatic control system in the transport and construction. Proc. scientific. tr. MADI. 86-92. (in Russian).
17. **Renman I., Ramar A., 1980.:** Perfomance Calculations of Induction Machines with a Solid Steel Rotor. Elec. Mach. and Electromech. #6. 509-521.

18. **Tatur T., 1989.:** Fundamentals of the theory of the electromagnetic field: a reference. allowance for electrotechnical. Specials. universities. M.: Higher. wk.. 271. (in Russian).
19. **Turovskii Ya., 1974.:** Technical Electrodynamics. Moscow: Energiya. 488. (in Russian).
20. **Verbovoy A., Verbovoy P., Sianov A., 1999.:** Investigation of the penetration depth of the electromagnetic wave in a massive electromagnetic rotor induction motor. Tehnicheskpya electrodynamics. № 1. 68-71. (in Russian).
21. **Zakharchuk I., 2007.:** Simulation of steady-state operation of the asynchronous motor with shielded fan shorting ring in the rotor windings dvuhpaketnogo. Visn. Shidnoukr. Nat. University. № 4 (110). 117-127. (in Russian).
22. **Zakharchuk I., 2011.:** Analysis of starting characteristics of asynchronous motor with shielded fan rings in the rotor winding. Visn. Shidnoukr. Nat. University. № 3 (157). 71-81. (in Russian).

МОДЕЛИРОВАНИЕ ЭЛЕКТРОМАГНИТНЫХ ПРОЦЕССОВ В ФЕРРОМАГНИТНЫХ ЭКРАНАХ КОРОТКОЗАМКНУТОЙ ОБМОТКИ АСИНХРОННОГО МОТОР-ВЕНТИЛЯТОРА С ДВУХПАКЕТНЫМ РОТОРОМ С ПОМОЩЬЮ ПРОГРАММНОГО КОМПЛЕКСА FEMM 3.4

Игорь Захарчук

А н н о т а ц и я . Определены активное и индуктивное сопротивления обмотки ротора путем моделирования электромагнитных процессов в ферромагнитных экранах короткозамкнутой обмотки асинхронного мотор-вентилятора с двухпакетным ротором с помощью программного комплекса FEMM 3.4.

К л ю ч е в ы е с л о в а : асинхронный мотор-вентилятор, моделирование электромагнитных процессов, ферромагнитные экраны.